

Improving the efficiency of learning-based error mitigation

Piotr Czarnik,^{1,2} Michael McKerns,³ Andrew T. Sornborger,³ and Lukasz Cincio^{1,4}

¹*Theoretical Division, Los Alamos National Laboratory, Los Alamos, NM, USA.*

²*Institute of Theoretical Physics, Jagiellonian University, Krakow, Poland.*

³*Information Sciences, Los Alamos National Laboratory, Los Alamos, NM, USA.*

⁴*Quantum Science Center, Oak Ridge, TN 37931, USA.*

Error mitigation will play an important role in practical applications of near-term noisy quantum computers. Current error mitigation methods typically concentrate on correction quality at the expense of frugality (as measured by the number of additional calls to quantum hardware). To fill the need for highly accurate, yet inexpensive techniques, we introduce an error mitigation scheme that builds on Clifford data regression (CDR). The scheme improves the frugality by carefully choosing the training data and exploiting the symmetries of the problem. We test our approach by correcting long range correlators of the ground state of XY Hamiltonian on IBM Toronto quantum computer. We find that our method is an order of magnitude cheaper while maintaining the same accuracy as the original CDR approach. The efficiency gain enables us to obtain a factor of 10 improvement on the unmitigated results with the total budget as small as $2 \cdot 10^5$ shots.

I. INTRODUCTION

Quantum computers have already demonstrated quantum advantage over classical computers [1, 2]. Nevertheless, current quantum computers suffer from significant levels of hardware noise which limits their computational power [3, 4]. At the same time, high noise levels and limited qubit counts make fault-tolerant quantum computing infeasible [5]. Consequently, to fully utilize the potential of near-term quantum computers, methods to approximately correct the effects of noise without performing quantum error correction are necessary [6, 7]. Such methods are called error mitigation methods [8].

Several approaches to error mitigation have been proposed. One of the most popular error mitigation approaches is Zero Noise Extrapolation, which, using a simple regression model, scales the noise strength in a controlled manner and then extrapolates to the zero noise limit [6, 9–15]. Another approach is probabilistic error cancellation which introduces additional gates to the executed circuit [9, 16]. The additional gates are introduced probabilistically according to the device noise model in order to cancel noise effects. An alternative approach is to use multiple copies of a noisy state to prepare its purification [17–24]. Such an approach is called Virtual Distillation. Other proposals are based on quantum phase estimation [25], symmetries of the mitigated system [26–29] or are unified methods bringing together different approaches to error mitigation [30–32]. Finally, circuit compilation methods can be used to reduce noise severity in combination with the error mitigation methods mentioned above [33–37]. Although many of these approaches have had success in small circuits, it remains to be seen which of them prove to be the most powerful in the quantum advantage regime.

Another recently proposed approach is learning-based error mitigation [38, 39], whose advantages we demonstrate in this work. Learning-based error mitigation learns the effects of noise from classically simulable quantum circuits which are close to non-simulable circuits of

interest. A large class of such approaches evaluates an observable’s expectation value for targeted training circuits on a quantum device using training data obtained classically. The training data are fitted with an ansatz capturing a relation between noisy and noiseless expectation values [38, 40–42]. The ansatz is used to correct the noisy expectation value for the circuit of interest. Learning-based error mitigation methods have been shown to perform well for quantum circuits with large qubit counts and depths [38, 43]. They have also been shown to outperform other state-of-the-art approaches [44]. The learning-based approach is a flexible framework which enables one to improve mitigation quality by expanding the training data to take into account the effects of varying noise strength on the expectation values of observables [44, 45]. These features make it a promising candidate for error mitigation for near-term quantum advantage applications.

One of the main limitations of error mitigation is the required shot cost [16]. In the case of learning-based error mitigation it has been shown that to maximize mitigation quality large shot resources are required [44, 45]. The required shot numbers seriously restrict the practical potential of most powerful and sophisticated approaches. Furthermore, instability in a quantum computer configuration that takes place over time introduces further limitations on the applicability and corrective power of error mitigation. Since quantum computers are effectively experimental apparatuses whose control parameters drift over time, training circuit data acquired over long times using many shots may not accurately reflect noise occurring during the execution of a circuit of interest. We show here that this effect is indeed strong enough to seriously affect error mitigation performance. Finally some of the most promising near-term applications like variational quantum algorithms require measurement of many quantum circuits to find a final circuit that forms a solution to the problem [8, 46]. To apply error mitigation methods to such problems one needs to optimize the shot-efficiency of the error mitigation approach [47].

In this work, we identify a major problem limiting the shot-efficiency of learning-based error mitigation. The most general and powerful learning-based error mitigation methods are based on learning from near-Clifford training circuits similar to the circuit of interest. Such training circuits are obtained by substituting non-Clifford gates in the circuit of interest by Clifford gates. We show that such a procedure leads to training circuits for which both noisy and exact expectation values of the observable of interest cluster around 0. We show that this effect leads to a large increase in the shot number necessary to learn the effects of noise on the observable of interest.

We propose two strategies to prevent clustering and improve the shot-efficiency of learning based error mitigation. First, we propose to generate near-Clifford training circuits with widely spread distributions of noisy and exact expectation values of the observable of interest using Markov Chain Monte Carlo sampling of near-Clifford circuits. We propose algorithms to generate such distributions which do not require quantum resources (shots) and therefore are suitable for improving the shot-efficiency.

Second, for circuits with symmetries we propose to use multiple observables, whose expectation values are equal by virtue of the symmetries, to increase the amount of training data available to learn the ansatz for noiseless expectation values. Such an increase enables us to learn from a fraction of the expectation values which are not clustered around 0. We show how to use this strategy to improve the shot-efficiency of error mitigation. We summarize schematically the proposed approaches in Fig. 1. To demonstrate the power of these strategies we mitigate correlation functions of the ground state of the XY model prepared using the IBM Toronto quantum computer. We obtain an order of magnitude improvement in mitigation quality over standard learning-based error mitigation for moderate mitigation shot costs of order 10^5 . Furthermore, for such shot costs, we find that the new method outperforms the standard one even when using a factor of 10 fewer shots.

In section II we describe a learning-based error mitigation method whose shot-effectiveness we improve here. Section III introduces the clustering problem and the strategies to improve shot-efficiency by alleviating it. Section IV discusses some benchmark results obtained for the IBM Toronto quantum computer and a noise model derived from IBM Ourense by gate tomography. We conclude and discuss possible extensions of this work in Section V. Technical details of a standard method of near-Clifford training circuit construction on which we improve here are described in Appendix A. In Appendix B we give details of our Markov Chain Monte Carlo algorithm for generating improved training circuits. Appendix C discusses the IBM Ourense derived noise model. In Appendix D we expand on the choice of hyperparameters for our IBM Toronto error mitigation implementation. Finally, in Appendix E we show evidence of the significant impact of hardware changes over time on per-

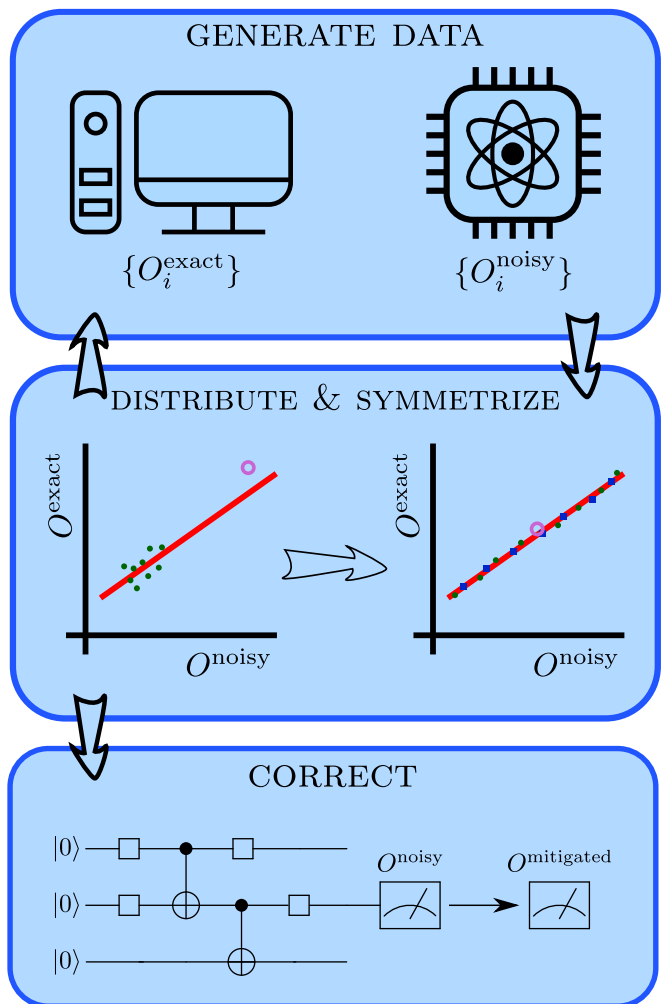


FIG. 1. **Improved Clifford Data Regression method.** Circuit of interest (denoted by \circ) together with observable O are used to generate training data $\{O_i^{\text{exact}}, O_i^{\text{noisy}}\}_i$ made out of observables computed from classically simulable circuits. They are evaluated on both, classical (O_i^{exact}) and noisy quantum (O_i^{noisy}) computers. Previous methods for generating training circuits resulted in data clustering, a situation in which the majority of training circuits share similar O^{exact} . This effect necessitates the use of large training data sets to maintain high quality correction $O^{\text{mitigated}}$. We solve that problem by distributing and symmetrizing the training data. Our approach significantly reduces the cost of data driven error mitigation techniques while preserving their high correction quality. Symmetries of the problem, if present, can be used to enhance the data further, i.e., to generate additional data (\blacksquare) from initially generated (\bullet) one, at no extra cost.

formance of error mitigation.

II. CLIFFORD DATA REGRESSION

Here, we work in the framework of Clifford Data Regression (CDR) [38]. CDR uses classically simulable near-Clifford circuits similar to a circuit of interest to

learn a linear ansatz that is used to mitigate an expectation value of a targeted observable for a circuit of interest. The method has been demonstrated to provide order-of-magnitude improvements in observable measurements for diverse applications [38, 43, 48] with real-world quantum hardware. The method consists of 4 steps outlined below.

1. Create N_t training circuits with N non-Clifford gates substituting non-Clifford gates in the circuit of interest by nearby Clifford gates. We describe a standard algorithm to generate the training circuits in Appendix A.
2. Evaluate an expectation value of the observable of interest O for each of the training circuits both classically and with a quantum computer. With this procedure, one obtains pairs of noisy O_i^{noisy} and exact expectation values O_i^{exact} for each training circuit.
3. Assume a linear relation between O^{exact} and O^{noisy} ,

$$O^{\text{exact}} = aO^{\text{noisy}} + b, \quad (1)$$

where a and b are given by

$$(a, b) = \operatorname{argmin} \sum_{i=1}^{N_t} (O_i^{\text{exact}} - aO_i^{\text{noisy}} - b)^2. \quad (2)$$

4. Use a and b found in step 3 to mitigate the expectation value O , for the circuit of interest

$$O_{\text{coi}}^{\text{mitigated}} = aO_{\text{coi}}^{\text{noisy}} + b. \quad (3)$$

III. IMPROVING EFFICIENCY OF LEARNING-BASED ERROR MITIGATION

A. Clustering of near-Clifford training circuits

The most general and widely used method for choosing training circuits for learning-based error mitigation, and CDR in particular, is to randomly replace most of the non-Clifford gates in the circuit of interest by nearby Clifford gates. We observe that for circuits of interest with a large number of non-Clifford gates this method results in the clustering of training data caused by the clustering of O^{exact} around 0. We visualize this effect in Fig. 2(a) for a typical training set obtained with the substitution method for a half-chain correlator of the ground state of an 8-qubit XY model using a noise model derived from gate tomography of IBM Ourense quantum computer.

As a thought experiment we consider the case of both training circuits and circuit of interest satisfying the CDR ansatz (1) perfectly. Then, the clustering of O^{exact} around 0 implies also clustering of O^{noisy} around 0. Consequently, a small number of training circuits results in similar values of O^{noisy} . Therefore, when we estimate O^{noisy} from a finite shot measurement, a much higher

number of shots is required to distinguish them than in the case when they are not clustered around a single value. If the number of shots is not large enough, coefficients of the fitted CDR ansatz are determined randomly by the shot noise making learning the correct CDR ansatz impossible. We find that this toy model explains the poor quality of CDR error mitigation for the case of the 8-qubit XY model and a typical standard training set obtained with small number of shots (2000 in this example). As we show in Figure 2(b), error bars of the finite shot estimates of O^{noisy} are so large that one can obtain nearly arbitrary CDR fit coefficients.

B. Distributing the training circuits

We observe that, despite the clustering of O^{exact} for near-Clifford circuits around 0, near-Clifford training circuits with large $|O^{\text{exact}}|$ can be found.

Based on this observation, we propose to use training circuits with a widely spread distribution of O^{exact} to improve the shot-efficiency of CDR. Such training circuits can be generated by post-selection of training circuits obtained with the standard algorithm or by Markov Chain Monte Carlo (MCMC) sampling of near-Clifford circuits. Both approaches require additional classical resources but they do not require any additional quantum resources.

Here, we use MCMC to generate training circuits with a wide and uniformly spaced O^{exact} distribution. See example in Fig. 2(a). We describe the method in detail in Appendix B. We find that our MCMC approach indeed significantly improves the quality of the CDR correction for modest shot requirements. The usefulness of the approach is demonstrated in Fig. 2(b) and by more extensive benchmarks in Section IV.

C. Enforcing symmetries of the system

Another strategy to improve shot efficiency in the presence of clustering is to exploit symmetries of the mitigated circuit. For certain types of symmetric systems, like those with translational symmetry, multiple observables have the same noiseless expectation values. Furthermore, multiple expectation values of such observables can typically be obtained from a single measurement of the circuit. Consequently, in such a case one can build training data for multiple symmetric observables using the same number of shots as for a single observable. In the presence of such symmetries, we propose to correct all symmetric observables with CDR while enforcing the constraint that all mitigated expectation values are the same. Using expectation values for many symmetric observables we increase the probability of including data points with large $|O^{\text{exact}}|$ and $|O^{\text{noisy}}|$ in our training data. The presence of training data with large $|O^{\text{noisy}}|$ improves the shot efficiency of CDR-based error mitiga-

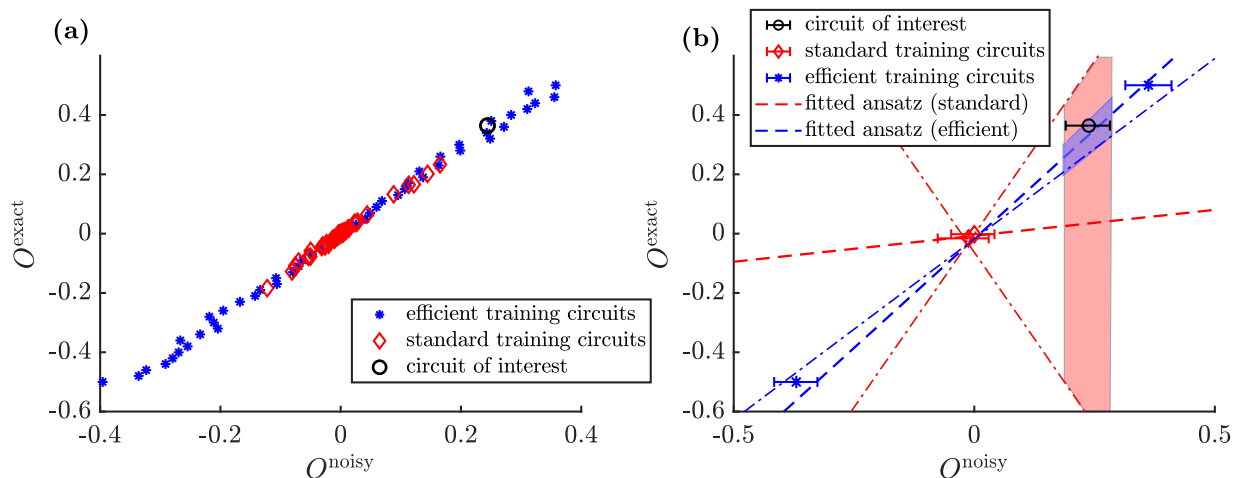


FIG. 2. **Improving CDR shot efficiency by distributing training circuits.** In (a) we show O^{exact} versus noisy O^{noisy} expectation values of a given observable computed from a circuit of interest as well as from CDR training circuits. The noisy expectation values were obtained in the limit of infinite shot number. We show results for two methods of training circuit construction. The results obtained with the standard method (random substitutions of non-Clifford gates by Clifford ones) are shown with red diamonds. They cluster around a $O^{\text{noisy}} = O^{\text{exact}} = 0$. The blue asterisks are results obtained for a set of training circuits with a wide distribution of O^{exact} generated by MCMC. This set also prevents clustering of O^{noisy} . In (b) we show the results of CDR error mitigation for a small shot cost. We use two training circuits generated by both methods. We evaluate 1000 shots to estimate O^{noisy} for both training circuits and the circuit of interest. Error bars correspond to 5th and 95th quantiles of O^{noisy} estimated from 100 shot noise instances, while the markers correspond to the median value. We performed CDR fits for all shot noise instances. We show CDR fits corresponding to 50th (dashed lines), 5th and 95th (dashed-dotted lines) quantiles of the mitigated expectation value. The shaded areas show confidence intervals of the mitigated expectation value based on statistical distribution of the fits. We see that CDR with distributed training circuits results in both smaller uncertainty and better quality of the mitigated expectation values. Thus, these results demonstrate that preventing clustering of the training data indeed improves the shot-efficiency of CDR error mitigation. Here, the circuit of interest approximates the ground state of an 8-qubit XY model (6) and $O = X_1 X_5$, where X is a Pauli matrix. To generate O^{noisy} we used a noise model described in Appendix C.

tion. By enforcing the constraint we ensure that such training data affects all mitigated expectation values.

An example of a circuit for which this approach can be applied is a circuit approximating an eigenstate of a translationally invariant Hamiltonian. For example, in the case of a translationally invariant one-dimensional Hamiltonian with periodic boundary conditions, noiseless observable expectation values

$$X_i X_{i'}, \quad i' = (i + l) \bmod Q, \quad i = 1, \dots, Q$$

are the same because of symmetry. Here, Q is the number of qubits, l is an integer and X_i is a Pauli matrix acting on qubit i . At the same time, for IBM quantum hardware, such expectation values can be measured simultaneously. Therefore, simultaneous CDR error mitigation is possible without requiring additional shot cost.

More formally we consider here the case of M observables with equal exact expectation values due to a symmetry of the mitigated system

$$O_1^{\text{exact}} = O_2^{\text{exact}} = \dots = O_M^{\text{exact}}.$$

We propose to create training data by measuring noisy expectation values of all observables for N_t training circuits and classically computing their corresponding exact

expectation values

$$\{(O_{ji}^{\text{exact}}, O_{ji}^{\text{noisy}})\}, \quad i = 1, \dots, N_t, \quad j = 1, \dots, M.$$

In a more general case one can also have different sets of training circuits for each observable (N_t may depend on observable index j).

We propose to find mitigated expectation values of these observables by fitting M linear ansaetze

$$O_j^{\text{exact}} = a_j O_j^{\text{noisy}} + b_j, \quad j = 1, \dots, M \quad (4)$$

to the training data. Their coefficients a_j, b_j are found by minimizing

$$\sum_{ij} (O_{ji}^{\text{exact}} - a_j O_{ji}^{\text{noisy}} - b_j)^2$$

under the constraint that the mitigated expectation values are equal:

$$a_1 O_{\text{coi},1}^{\text{noisy}} + b_1 = \dots = a_M O_{\text{coi},M}^{\text{noisy}} + b_M. \quad (5)$$

Such a constrained optimization can be performed with the mystic package [49, 50]. We show an example of the shot-efficiency improvement with this approach in Fig. 3.

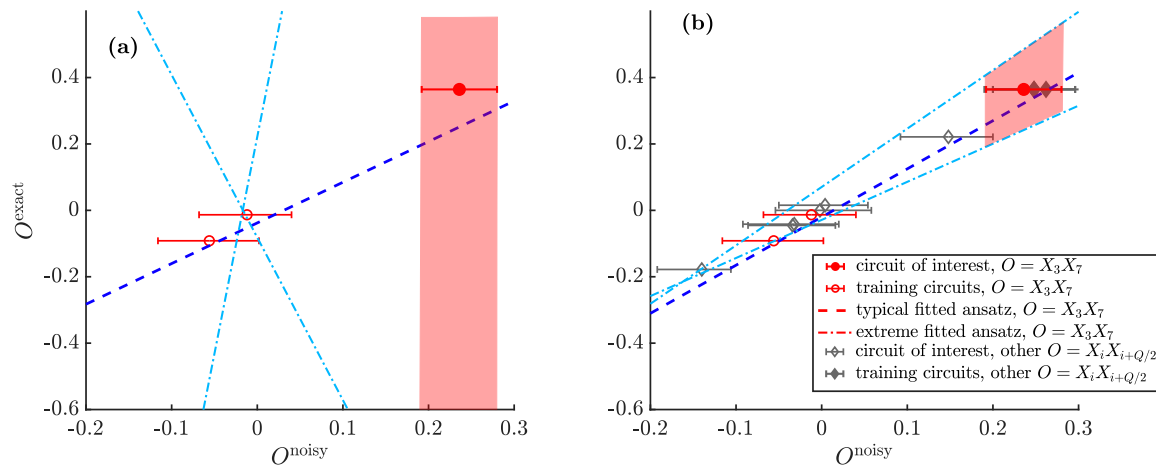


FIG. 3. **Improving CDR shot efficiency by enforcing symmetries of the mitigated circuit.** We perform CDR error mitigation for the ground state of 8-qubit XY model with periodic boundary conditions simulated with the IBM Ourense noise model. We mitigate the expectation value of $O = X_3X_7$ for the ground state using two training circuits generated by the standard substitution algorithm and performing 1000 shots for each circuit. In (a), we show results of standard CDR error mitigation. As in Figure 2(b), we find that expectation values of the training circuits (red circles) cluster around (0,0) and that due to the clustering, the uncertainty of the mitigated expectation value shown by the red shaded area is large. We visualize this effect performing CDR error mitigation for 100 instances of shot noise. (The shot noise is represented by the error bars of O^{noisy} in the same way as in Figure 2(b)). We show typical and extreme CDR fits (defined as in Figure 2(b)) with the blue line and the cyan lines, respectively. In (b), we take advantage of the translational invariance of the ground state which implies that $X_1X_5, X_2X_6, X_3X_7, X_4X_8$ all have the same noiseless expectation values. We measure all of these observables for both our circuit of interest and the training circuits. They are mitigated simultaneously imposing equality of their mitigated expectation values. The additional observables (induced by symmetry) are shown as gray diamonds in the plot. We correct 100 different shot noise instances of the noisy expectation values and show the fits corresponding to typical and extremal mitigated expectation value of X_3X_7 . We find that uncertainty of the mitigated expectation value and quality of the typical CDR fit are significantly improved with respect to (a). For the sake of transparency we do not show the CDR fits for other observables. They have similar quality to the ones shown here.

While in this section we concentrate on application of symmetric CDR to improve shot-efficiency of error mitigation, it can be also used to enforce symmetries of the mitigated circuit for the mitigated expectation values. Such symmetries are usually broken by the noise, therefore the standard CDR is not guaranteed to restore them.

IV. BENCHMARK RESULTS

A. The ground state of an XY model

We test the proposed methods for the ground state of a one-dimensional XY model with periodic boundary conditions given by a Hamiltonian

$$H = \sum_{\langle i,j \rangle} X_i X_j + Y_i Y_j. \quad (6)$$

Here X_i and Y_i are Pauli matrices acting on qubit i and N is the number of lattice sites, or required qubits, in the model. This Hamiltonian has a translational symmetry and it preserves the Hamming weight, i.e. it has a $U(1)$ symmetry.

We use the Variational Quantum Eigensolver [51] to prepare the ground state for $Q = 6, 8$ with a noiseless

classical simulator and enforced translational symmetry. We employ a hardware efficient ansatz with sufficient number of layers such that the energy of the prepared state matches the exact ground state energy with accuracy better than 10^{-13} .

Here we mitigate error of expectation values of long range correlators for the ground state of the model. Because of the symmetries of the ground state we have N identical half-chain correlators:

$$\begin{aligned} O_j &= X_j X_{Q/2+j}, & 1 \leq j \leq Q/2, \\ O_j &= Y_{j-Q/2} Y_j, & Q/2+1 \leq j \leq Q, \end{aligned} \quad (7)$$

with equal noiseless expectation values. Below we mitigate the errors of expectation values of these observables making use of the spreading and symmetry properties outlined above.

B. Implementation on quantum hardware

We mitigate half-chain correlators (7) of the $Q = 6$ XY model (6) using IBM's Toronto quantum computer. As a reference, we also perform CDR correction with a standard algorithm described in Section II and Appendix A using training circuits obtained via random Clifford sub-

stitutions. Our current shot-efficient CDR method combines both approaches described in Section III. Namely, we perform symmetric CDR for all O_j in (7) following the algorithm of Section III C. Each symmetric observable O_j requires generating independent N_t^j training circuits with widely spread O_j^{exact} . These training circuits are generated using the MCMC algorithm described in Appendix B. We describe construction of the training sets for both approaches in more detail in Appendix D. The shot-frugal approach used here improves CDR shot-efficiency through spreading O_j^{exact} , while symmetric CDR restores uniformity of the mitigated correlators. One may consider generalizations of the MCMC algorithm which would allow one to generate training circuits with distributions of several O_j^{exact} being widely-spread simultaneously. Such training circuits would improve shot-efficiency of the current approach while increasing classical computational cost of the method. We leave their investigation to future work.

We compare the performance of the new and standard approaches using IBM’s Toronto quantum computer. We use $N_s = 10^4$ shots per circuit measurement and compare the performance of both approaches for a total number of training circuits $N_t = 2, 6, 8, 12, 18, 30$. For each value of N_t we generate 10 different, independent instances of training circuits. The number of non-Clifford gates is set to $N = 30$, while the circuit of interest contains 150 non-Clifford gates. We compare the performance by computing the absolute error of the mean of the observable expectation values for each set of training circuits

$$\text{absolute error} = \left| \sum_j (O_j^{\text{noisy/mitigated}} - O_j^{\text{exact}}) \right|. \quad (8)$$

For both methods, we compare mean and maximal absolute errors obtained for a given N_t from a sample of 10 sets of training circuits. To further randomize results for each set of training circuits we perform independent measurements of the circuit of interest. We gather the results and plot them versus total shot cost of the mitigation, N_s^{tot} , in Figure 4.

Figure 4 shows data acquired with standard and efficient CDR methods. We concentrate on the realistic regime of $N_s^{\text{tot}} \in [3 \cdot 10^4, 3.2 \cdot 10^5]$ and show maximum and minimum errors obtained with both methods. We observe that the new efficient CDR method displays better performance as well as faster convergence with increasing N_s^{tot} . These results show a substantial improvement of up to an order of magnitude for the new, efficient method. Importantly, efficient CDR reaches its correction capabilities already at small shot budgets. This makes it a preferable tool for applications that require the execution of many different quantum circuits. This is a typical situation in many approaches involving variational quantum algorithms.

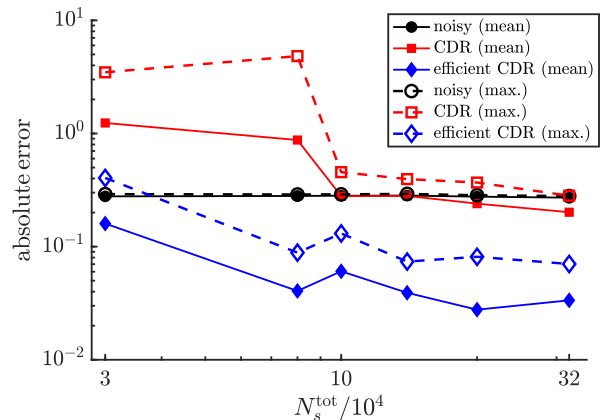


FIG. 4. **Benchmark results for IBM Toronto.** We compare standard and efficient CDR performance for the ground state of the $Q = 6$ qubit XY model (6) by mitigating symmetric half-chain correlators (7) of the ground state. The comparison is performed for $N_s = 10^4$ shots per circuit measurement and $N_t = 2, 6, 8, 12, 18, 30$ training circuits. For each N_t and each CDR version we construct 10 independent sets of training circuits, see details in Section IV B and Appendix D. Furthermore, for each set we carried out independent measurements of the circuit of interest. For each training set we perform error mitigation and quantify its quality by computing absolute error of the correlators (8). For each method and each N_t value we determine the maximal and the mean absolute error of the mitigated correlators for the sample of training circuits. We plot these errors versus total shot cost N_s^{tot} . For a reference we also plot the errors of unmitigated, raw results (black lines). We observe that shot-efficient CDR displays up to an order-of-magnitude correction improvement over the standard method and faster convergence of the mitigated observables with increasing N_s^{tot} .

C. Quantum computer noise model

We perform a more detailed benchmark using a noise model obtained by performing full process tomography of basic gates available on IBM’s Ourense quantum computer. Namely, we additionally examine the effect of varying N_s on the performance of shot-efficient CDR. Furthermore, we analyze larger Q and gather better statistics using larger samples of training circuits. The noise model is described in detail in Appendix C. Taking into account that the device is an early generation, already retired quantum computer and that we mitigate circuits with larger Q and depth than in the case of our real-hardware implementation we reduced gate error rates in the model by a factor of 10 with respect to the original Ourense noise model. This allows us to perform the analysis for noise strengths for which basic CDR provide good quality of error mitigation. While current quantum computers may have noise strengths larger than assumed here, we expect that improvements in quantum computing architectures will reduce the error rates in the near-future.

As in the case of our implementation on IBM’s Toronto

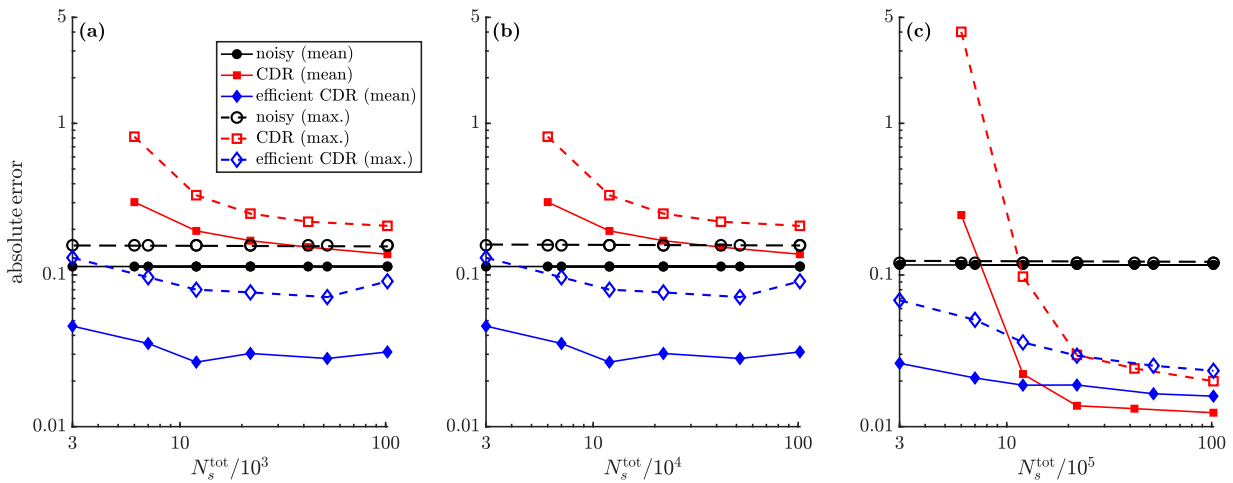


FIG. 5. **Benchmark results for a noise model.** Comparison of the standard (red curves) and efficient (blue curves) CDR for the ground state of $Q = 8$ qubit XY model (6) by mitigating symmetric half-chain correlators (7) of the ground state. We use a noise model described in detail in Appendix C. The performance is compared for $N_s = 10^3$ (a), $N_s = 10^4$ (b) and $N_s = 10^5$ shots (c) per a circuit measurement and $N_t = 2 - 100$ training circuits. For each N_t and each CDR version we construct 50 independent sets of training circuits. They are obtained in the same way as for IBM Toronto error mitigation, see Section (IV B). Circuit of interest is measured independently in each set. We plot mean and maximal absolute errors (8) of both CDR methods and the noisy data versus total shot cost of the error mitigation N_s^{tot} . We observe that the shot-efficient version significantly outperforms the standard one for small and moderate total shot costs $N_s^{\text{tot}} = 3 \cdot 10^3 - 1.2 \cdot 10^6$.

processor, we mitigate symmetric half-chain correlators (7) of the ground state of the XY model with periodic boundary conditions (6). We choose $Q = 8$. We compare the performance of shot-efficient and standard algorithms using the same set-up as for the IBM Toronto benchmark in Section IV B. This time we consider three different values of $N_s = 10^3, 10^4, 10^5$ and a larger range of $N_t = 2 - 100$. Such choice enables us to test the shot-efficient method for large error mitigation total shot costs. Additionally, for each value of N_t and for each method, we generate 50 independent sets of training circuits instead of 10 to decrease finite sample effects. It is currently not possible to perform those extended experiments on real quantum computers due to hardware drift. We discuss those issues in more detail in Appendix E. Effects caused by hardware drift further motivate shot-efficient error mitigation techniques.

We gather the results (the mean and the maximal errors evaluated from a sample of 50 sets of training circuits) and plot them versus N_s^{tot} in Figure 5. Results obtained with $N_s = 10^3, 10^4$ resemble those observed on the real device. Namely, even in the limit of large N_t we see that the shot-efficient algorithm outperforms standard CDR algorithm. At the same time, we notice that the shot-efficient mitigated results converge much faster with increasing N_s^{tot} than the standard mitigated ones. For $N_s = 10^5$ we again see much faster convergence of the shot-efficient CDR which outperforms the standard version for $N_s^{\text{tot}} \leq 1.2 \cdot 10^6$. Standard CDR slightly outperforms the shot-efficient version for the largest $N_s^{\text{tot}} \geq 2.2 \cdot 10^6$.

Overall, we observe that for small and moderate shot

costs (up to $1.2 \cdot 10^6$), the shot-efficient CDR outperforms the standard algorithm. For example, efficient CDR provides improvement of the mitigated results over the noisy ones consistently for all $N_s^{\text{tot}} \geq 3 \cdot 10^3$. This should be compared with standard CDR that shows improvement only for much larger total budgets, $N_s^{\text{tot}} \geq 1.2 \cdot 10^5$. Thus, efficient CDR improves that shot budget threshold by almost two orders of magnitude. Similarly, the shot-efficient method obtains improvement by a factor of at least 4 with respect to the noisy results for all $N_s^{\text{tot}} \geq 7 \cdot 10^4$. The standard CDR method requires at least $N_s^{\text{tot}} = 1.2 \cdot 10^6$ to reach similar improvement.

V. CONCLUSIONS AND DISCUSSION

We proposed methods to improve the shot-efficiency of CDR. Our new methods rely on the observation that for large and deep circuits, the expectation values of near-Clifford circuits used by CDR to learn the noise effects cluster around 0. Because of that effect, a large number of shots is required to distinguish noisy expectation values. Consequently, a large number of shots is necessary to learn the correction successfully.

We proposed two strategies to alleviate this effect. The first one is to generate a distribution of near-Clifford training circuits with widely distributed exact expectation values for the circuit of interest. We show that such a distribution can be generated with Markov Chain Monte Carlo sampling (MCMC) without requiring any quantum resources.

The second strategy is to exploit symmetries of the

mitigated system by identifying multiple observables which by virtue of the symmetry have the same expectation values and can be measured simultaneously. In the presence of such symmetries, we propose that one performs CDR correction simultaneously for all observables by enforcing the symmetric constraint. This procedure effectively increases the number of available data points to optimize the CDR ansatz. It also restores symmetries of the error mitigated expectation values of the observables.

We have demonstrated that both strategies can be used to improve CDR shot-efficiency. We combined the strategies and applied them for error mitigation of the ground state of the XY Hamiltonian. This model displays translational and U(1) symmetries. The latter one is responsible for Hamming weight preservation.

Using IBM Toronto we have demonstrated an order-of-magnitude improvement in shot-efficiency relative to standard CDR for moderate total shot costs ($3 \cdot 10^4 - 3 \cdot 10^5$). Furthermore, we analyzed the performance of our shot-efficient method in more detail for an IBM Ourense-based noise model and found consistent improvement of our new method over standard methods for a large range of total error mitigation shot costs ($3 \cdot 10^3 - 10^6$).

The clustering problem affects all error mitigation methods that learn from near-Clifford circuits including vnCDR and UNITED. We expect that our proposed strategies will improve the shot-efficiency of these methods as well. The above techniques have been shown to require more shots than CDR to obtain substantial improvement over CDR. Therefore, improvements of their shot efficiency will be crucial for their practical application.

An additional important question is how the classical resources (e.g. the cost of the MCMC algorithm) required to obtain an informative distribution of training circuits scale with size and other parameters of the system. Here we performed benchmark simulations for symmetric systems exploiting symmetries of the mitigated system. Further investigation will be necessary to test the performance of the method when there are no symmetries to exploit.

Finally, it will be interesting to study the extent to which the proposed techniques affect the performance of CDR in the limit of large shot number. In particular, the symmetric CDR algorithm, apart from improving the shot-efficiency, restores symmetries of the mitigated system restricting possible error mitigation outcomes. A question arises whether such a restriction can improve the quality of error mitigation for degrees of freedom not fixed by the symmetry.

Similarly, the usage of distributed training circuits in the limit of large shot number requires further examination. It has been observed that in some cases the use of training circuits with mitigated observable distribution close to the expectation value of the circuit of interest improves the quality of CDR corrections [38] in comparison to the standard Clifford method. It remains to be

seen if this effect occurs for the training circuit distributions proposed here.

ACKNOWLEDGMENTS

We thank Mike Martin for insightful discussions. PC acknowledges initial support from Laboratory Directed Research and Development (LDRD) program of Los Alamos National Laboratory (LANL) under project numbers 20190659PRD4 with subsequent support by the National Science Centre (NCN), Poland under project 2019/35/B/ST3/01028. MM and ATS acknowledge initial support from the Los Alamos National Laboratory (LANL) ASC Beyond Moore's Law project with subsequent support by the Laboratory Directed Research and Development (LDRD) program of Los Alamos National Laboratory under project number 20210116DR. This material is based upon work supported by the U.S. Department of Energy, Office of Science, National Quantum Information Science Research Centers, Quantum Science Center (LC). LC was also initially supported by the U.S. DOE, Office of Science, Office of Advanced Scientific Computing Research, under the Quantum Computing Application Teams program. This research used resources provided by the Los Alamos National Laboratory Institutional Computing Program, which is supported by the U.S. Department of Energy National Nuclear Security Administration under Contract No. 89233218CNA000001.

Appendix A: Training circuit generation - standard algorithm.

Here we outline an algorithm to generate CDR training circuits used as a reference in the main text. The algorithm is based on random substitution of non-Clifford gates in a circuit of interest by nearby Clifford gates. The algorithm was originally proposed in [38] and was used and incorporated in subsequent error mitigation frameworks [45, 47]. Here we present it for a circuit compiled with native IBM gates X , \sqrt{X} , $R_Z(\theta)$ and CNOT.

X , \sqrt{X} and CNOT are Clifford gates while $R_Z(\theta) = e^{-i\theta/2Z}$ is a Clifford gate only for $\theta = k\pi/2$, where k is an integer. Therefore, for a circuit containing \tilde{N} non-Clifford R_Z gates we replace $\tilde{N} - N$ R_Z gates by Clifford R_Z rotations to obtain a training circuit with N non-Clifford gates. We denote angles of the non-Clifford rotations by $\theta_i, i = 1, \dots, \tilde{N}$. We replace these gates using the following procedure:

1. Take the circuit of interest as an input circuit. Repeat steps 2 and 3 $\tilde{N} - N$ times.
2. For each non-Clifford gate $R_Z(\theta_i)$ in the input circuit, calculate weights $w_{ik} = e^{-d_{ik}^2/\sigma^2}$, $k = 0, 1, 2, 3$. Here, $d_{ik} = \|e^{i\theta_i/2}R_Z(\theta_i) - e^{ik\pi/4}R_Z(k\pi/2)\|_F$,

$\|\cdot\|_F$ is the Frobenius matrix norm and σ is a parameter. Note that d_{ik} quantifies the distance between $R_Z(\theta_i)$ and $R_Z(k\pi/2)$ in a way which does not depend on any global phase introduced by the action of these gates. We choose $\sigma = 0.5$ following [38, 45, 47].

3. Replace a gate $R_Z(\theta_i)$ by $R_Z(k\pi/2)$ according to the probability distribution

$$p_{ik} = \frac{w_{ik}}{\sum_{i=1}^m \sum_{k=0}^3 w_{ik}}, \quad (\text{A1})$$

where m is the number of non-Clifford gates in the input circuit, generating an output circuit. If it contains more than N non-Clifford gates, take it as an input circuit for the next repetition of step 2.

4. Take the final output circuit as the training circuit.

Appendix B: Training circuit generation - efficient algorithm.

Here we present an algorithm to generate a distribution of training circuits with widely distributed values of O^{exact} used by the shot-efficient CDR method. The algorithm attempts to generate training circuits with values of O^{exact} close to target values y_1, y_2, \dots, y_n using Markov Chain Monte Carlo (MCMC) sampling [52] of near-Clifford circuits. For each target value, y_k , we generate an MCMC chain built from near-Clifford circuits with N non-Clifford gates using a target probability distribution $p \propto e^{-(O^{\text{exact}} - y_k)^2 / \sigma_{\text{MCMC}}^2}$ where O^{exact} is the exact expectation value of the mitigated observable for a near-Clifford circuit and σ_{MCMC} is a constant. We select a circuit with O^{exact} close to y_k as a training circuit. In this work, O is a Pauli string and we choose $y_i = -0.5 + \frac{i-1}{n-1}$, $i = 1, 2, \dots, n$. For this choice, we have a distribution of target values $|y_n - y_1| = 1$ which is comparable to the maximal possible spread of O^{exact} (i.e. 2). Furthermore, we choose $\sigma_{\text{MCMC}} = 0.01$.

We use a version of the Metropolis-Hastings algorithm [52] to generate an MCMC chain for a given y_k . We assume here that near-Clifford circuits in the chain can be obtained by replacing most of the non-Clifford gates in the circuit of interest by Clifford gates and consequently the circuit of interest can be obtained by replacing some of the Clifford gates in circuits from the chain by non-Clifford gates. The algorithm is:

1. Initialize the chain taking as its first element a near-Clifford circuit with N non-Clifford gates obtained by substituting most of non-Clifford gates in the circuit of interest by Clifford gates. In our implementation, we use an algorithm from Appendix A to generate the first circuit. Repeat steps 2 and 3 until a circuit with O^{exact} close enough to y_k is generated.

2. Prepare a candidate circuit by taking the last circuit of the chain and replacing N_g randomly chosen non-Clifford gates by Clifford gates and N_g randomly chosen Clifford gates by the corresponding non-Clifford gates of the circuit of interest. Note that the new circuit has N non-Clifford gates which are the same as corresponding non-Clifford gates in the circuit of interest.

3. Compute the ratio $w_{\text{cand}}/w_{\text{accept}}$, where

$$w_{\text{cand}} = e^{-(y_{\text{cand}} - y_k)^2 / \sigma_{\text{MCMC}}^2}, \quad (\text{B1})$$

$$w_{\text{accept}} = e^{-(y_{\text{accept}} - y_k)^2 / \sigma_{\text{MCMC}}^2} \quad (\text{B2})$$

and $y_{\text{cand}}, y_{\text{accept}}$ are O^{exact} for the new circuit and the last circuit of the chain, respectively. Generate a random number $u \in [0, 1]$. If $u < w_{\text{cand}}/w_{\text{accept}}$, accept the new circuit as the last circuit of the chain. Otherwise add a copy of the last circuit to the chain.

In the limit of long MCMC chains this algorithm is guaranteed to generate a distribution of near-Clifford circuits converging to the target distribution $p \propto e^{-(O^{\text{exact}} - y_k)^2 / \sigma_{\text{MCMC}}^2}$ [52].

We implement step 2 setting $N_g = 5$ and replace $R_Z(\gamma)$ by $R_Z(k\pi/2)$ according to a probability distribution

$$p_k = \frac{w_k}{\sum_{k=0}^3 w_k}, \quad w_k = e^{-d_k^2 / \sigma^2}, \quad (\text{B3})$$

$$d_k = \|e^{i\theta/2} R_Z(\theta) - e^{ik\pi/4} R_Z(k\pi/2)\|_F.$$

Here, we set $\sigma = 0.5$. We find that such implementation results in fast convergence of the MCMC chains to the target distribution.

Appendix C: The noise model

We construct the noise model used in Section IV C with process matrices obtained by gate set tomography (GST) experiments performed on the IBM Oursense quantum computer. These matrices are given in Appendix B of [53], where the details of the experiments can be found. Our goal in Section IV C is to investigate shot-efficiency gains for deep circuits that are challenging to mitigate with current hardware. To achieve that, we reduce the effective noise rates of the model in comparison to the original process matrices' noise rates. Such a reduction is further justified by the fact that IBM Ourens's noise rates are higher than the error rates of current IBM quantum computers. Furthermore, in our noise model we assume that the noise rates of gates vary for different qubits and different connections between qubits as in the case of real devices.

More explicitly, in our noise model we assume (following [53]) that native gates of the device are $R_X(\pi/2) =$

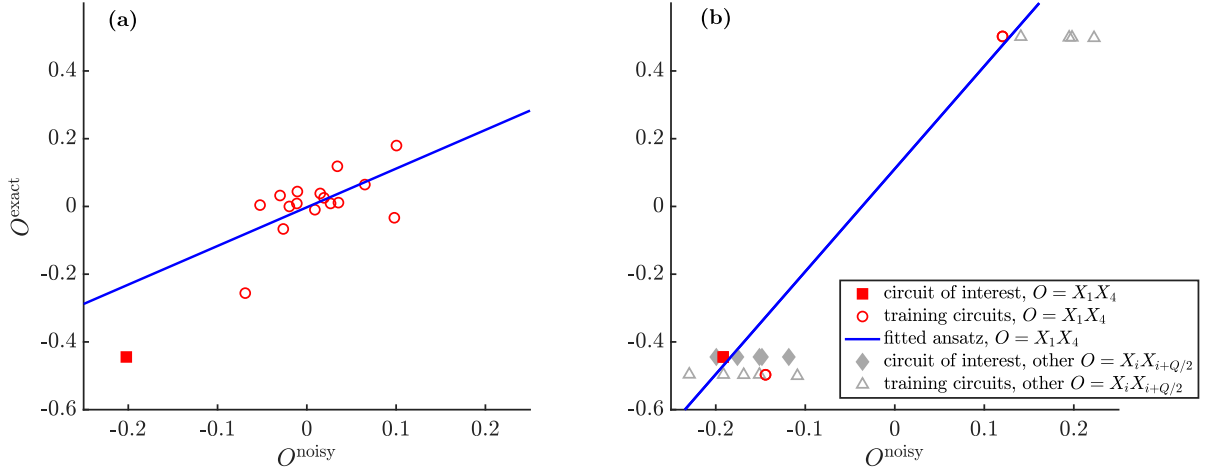


FIG. 6. **Training sets from the real-hardware implementation.** In (a), we show a standard CDR training set for the real-hardware implementation from Figure 4 and the ground state expectation value of X_1X_4 (red square). Here we use 15 training circuits (red circles) to correct X_1X_4 . Number of shots per expectation value evaluation is $N_s = 10^4$. Due to clustering of the training circuits quality of the CDR mitigation is poor as shown by the fitted CDR ansatz (blue line). We obtained similar results for other correlators (7). In (b), we show a training set for the shot-efficient method and $N_t = 12$. Here we correct all symmetric half-chain correlators (7) using the symmetric CDR algorithm and generate a widely-spread distribution of the training circuits for each observable independently. Red squares and circles show expectation values of X_1X_4 for the training data and the circuit of interest. Gray squares and circles show expectation values of the other symmetric correlators. As in (a), we have $N_s = 10^4$. We obtain good quality of the error mitigation despite total shot cost of the error mitigation N_s^{tot} being smaller than in (a). For the sake of transparency we show a CDR fit only for X_1X_4 . For other correlators (7), quality of the error mitigation is similar.

$e^{-i\pi/4X}$ (which is equivalent up to the global phase \sqrt{X}), CNOT, identity I and $R_Z(\alpha) = e^{-i\alpha/2Z}$. R_Z is assumed to be perfect as is the case for IBM quantum computers. We construct process matrices of I and $R_X(\pi/2)$ as convex combinations of the processes matrices from [53] $R_X(\pi/2)^{\text{Ourense}}, I^{\text{Ourense}}, \text{CNOT}^{\text{Ourense}}$ and the noiseless process $R_X(\pi/2)^{\text{perfect}}, I^{\text{perfect}}, \text{CNOT}^{\text{perfect}}$

$$R_X(\pi/2)^i = p_i R_X(\pi/2)^{\text{Ourense}} + (1 - p_i) R_X(\pi/2)^{\text{perfect}}, \quad (\text{C1})$$

$$I^i = p_i I^{\text{Ourense}} + (1 - p_i) I^{\text{perfect}}, \quad (\text{C2})$$

$$\text{CNOT}^{ij} = p_{ij} \text{CNOT}^{\text{Ourense}} + (1 - p_{ij}) \text{CNOT}^{\text{perfect}}. \quad (\text{C3})$$

Here, indices i and j number qubits and p_i, p_{ij} were drawn randomly from a uniform probability distribution on the interval $[0.05, 0.15]$. Consequently, the error rates are on average reduced with respect to noise rates of the IBM Ourense approximately by a factor of 10.

Furthermore, we assume the presence of state preparation error. We assume that the initial state ρ_0 is a product state of single-qubit states

$$\rho_0 = \rho_0^1 \otimes \cdots \otimes \rho_0^N \quad (\text{C4})$$

with

$$\rho_0^i = p_i \rho_0^{\text{Ourense}} + (1 - p_i) \rho_0^{\text{perfect}}, \quad (\text{C5})$$

where ρ_0^{Ourense} corresponds to the initial state obtained by GST experiments for IBM Ourense and given in Appendix B of [53], while ρ_0^{perfect} corresponds to perfect state preparation. In our noise model we neglect measurement error as it can be efficiently mitigated by specialized techniques [54–56]. p_i were drawn randomly from a uniform probability distribution on the interval $[0.05, 0.15]$.

Appendix D: Training sets from the real-hardware implementation

For the standard CDR we generate training circuits by random substitutions as described in Appendix A. We measure the circuit of interest in one basis to determine expectation values of $O_i = X_iX_{i+Q/2}$, $i = 1, \dots, Q/2$ correlators and in another one to determine expectation values of $O_{i+Q/2} = Y_iY_{i+Q/2}$, $i = 1, \dots, Q/2$ correlators. We consider cases of $N_t = 2, 6, 8, 12, 30$ training circuits to correct O_i^{noisy} . To gather statistics for each case we generate 10 independent sets of training circuits. As we need to measure $X_iX_{i+Q/2}$ and $Y_iY_{i+Q/2}$ independently, for $N_t > 2$ we measure randomly chosen $N_t/2$ circuits in the $X_iX_{i+Q/2}$ basis and another half of the training circuits in the $Y_iY_{i+Q/2}$ basis. This strategy cannot be used for $N_t = 2$, so in that case for half of the sets of the training circuits we measure $X_iX_{i+Q/2}$ correlators and for the other half $Y_iY_{i+Q/2}$ correlators. To randomize the results further, while performing CDR correction for each set of

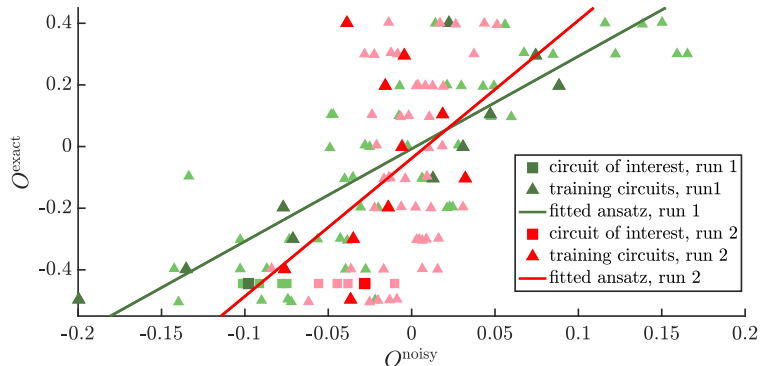


FIG. 7. **Effects of the hardware drift.** We compare two shot-efficient CDR runs conducted for the same circuit of interest at two different times. We mitigate the half-chain correlators (7) of the ground state of the 6-qubit XY model using IBM Toronto. Run number 1 was conducted on 01/22/2022 while run number 2 was performed on 03/23/2022. In both runs we used the same training circuits which were compiled to the native gates in the same way. We show here training sets and fitted ansaetze from both runs. Green squares and triangles are the results from the run number 1 while the red ones are results from run 2. We use dark red and dark green symbols to show X_1X_4 and light red and light green ones to plot the other correlators (7). The drift changed distribution of O^{noisy} affecting parameters of the fitted ansaetze and quality of CDR mitigation. Here, for the sake of transparency we plot only CDR fits (the lines) for X_1X_4 . The fits for other correlators give similar quality of the correction as the ones shown here. For the run 1 we obtain the mitigated error 0.14 while for the run 2 the mitigated error is 0.28. We remark that here quality of the error mitigation is in both cases worse than the one reported in Figures 4, 6 as we use 6 of 27 qubits of the device with larger error rates than the ones used in Figures 4, 6.

the training circuits, we measure the circuit of interest independently. Figure 6(a) shows a typical (resulting in median value of the mitigated error (8)) training set generated by that procedure for $O_1 = X_1X_4$ and $N_t = 30$, $N_s = 10^4$. Obtained training sets are strongly affected by clustering of the training circuits in the same way as in the case of training sets generated with the noise model in Figure 2. That explains poor performance of the standard CDR.

In the case of the shot-efficient version we generate distributions of widely-distributed training circuits for each O_i independently. To that end we use an algorithm from Appendix B. In the case of $N_t = 12, 18, 30$ for each O_i we generate training circuits with values of $O_i^{\text{exact}} \approx -0.5, 0.5$, $O_i^{\text{exact}} \approx -0.5, 0., 0.5$, and $O_i^{\text{exact}} \approx -0.5, -0.25, 0, 0.25, 0.5$, respectively. For $N_t < 12$ we choose randomly $N_t/2$ observables O_i for which we generate the training circuits with $O_i^{\text{exact}} \approx -0.5, 0.5$. To randomize results for each N_t we consider 10 different sets of training circuits obtained by starting MCMC chains with different initial circuits. Additionally, for each set of training circuits we use independent measurements of the circuit of interest. We show a typical training set for $N_t = 12$ in Figure 6(b).

Appendix E: Effects of hardware drift on performance of learning-based error mitigation

Shot-efficiency of the error mitigation is crucial for obtaining good quality of quantum computation when shot

resources are limited. Here we argue that shot resources are not only limited by available time of a quantum computer. They are also effectively limited by its variability in time. In the case of the learning-based error mitigation we learn the correction from training circuits assuming that the noise remains constant in time. That assumption is an idealization of real-world devices. In reality, certain characteristics of such devices “drift” in time. The shot-efficient method proposed here enables to perform the error mitigation over a shorter period of time than the standard method. Therefore, it violates the constant noise assumption less severely than the standard CDR method. Consequently, we expect it to deliver better quality of the error mitigation than the standard approach. While we leave quantifying this effect to a future work, we show a proof of principle results demonstrating that the drift affects the quality of the error mitigation. Namely, we performed shot-efficient CDR error mitigation for the symmetric half-chain correlators (7) of the ground state of the 6-qubit XY model using IBM Toronto at two different times. In both cases we used the same training circuits which we compiled to the native gates in the same way. We found that coefficients of the fitted CDR ansaetze and average quality of the error mitigation are different for those two runs, see Figure 7. For the run number 1 which occurred on 03/23/2022 we obtained the mitigated error 0.14. For the run number 2 which was conducted on 01/22/2022 we obtained the mitigated error 0.28. Mitigated errors are computed according to (8). That comparison shows that, indeed, the device drift can significantly alter results of the error mitigation.

-
- [1] Frank Arute, Kunal Arya, Ryan Babbush, Dave Bacon, *et al.*, “Quantum supremacy using a programmable superconducting processor,” *Nature* **574**, 505–510 (2019).
- [2] Han-Sen Zhong, Yu-Hao Deng, Jian Qin, Hui Wang, *et al.*, “Phase-programmable gaussian boson sampling using stimulated squeezed light,” *Phys. Rev. Lett.* **127**, 180502 (2021).
- [3] Samson Wang, Enrico Fontana, Marco Cerezo, Kunal Sharma, Akira Sone, Lukasz Cincio, and Patrick J Coles, “Noise-induced barren plateaus in variational quantum algorithms,” *Nature Communications* **12**, 1–11 (2021).
- [4] Daniel Stilck França and Raul Garcia-Patron, “Limitations of optimization algorithms on noisy quantum devices,” *Nature Physics* **17**, 1221–1227 (2021).
- [5] Sitan Chen, Jordan Cotler, Hsin-Yuan Huang, and Jerry Li, “Exponential separations between learning with and without quantum memory,” *arXiv preprint arXiv:2111.05881* (2021).
- [6] Abhinav Kandala, Kristan Temme, Antonio D. Córcoles, Antonio Mezzacapo, Jerry M. Chow, and Jay M. Gambetta, “Error mitigation extends the computational reach of a noisy quantum processor,” *Nature* **567**, 491–495 (2019).
- [7] Ryan LaRose, Andrea Mari, Vincent Russo, Dan Strano, and William J. Zeng, “Error mitigation increases the effective quantum volume of quantum computers,” *arXiv preprint arXiv:2203.05489* (2022).
- [8] Suguru Endo, Zhenyu Cai, Simon C Benjamin, and Xiao Yuan, “Hybrid quantum-classical algorithms and quantum error mitigation,” *Journal of the Physical Society of Japan* **90**, 032001 (2021).
- [9] Kristan Temme, Sergey Bravyi, and Jay M. Gambetta, “Error mitigation for short-depth quantum circuits,” *Phys. Rev. Lett.* **119**, 180509 (2017).
- [10] Eugene F Dumitrescu, Alex J McCaskey, Gaute Hagen, Gustav R Jansen, Titus D Morris, T Papenbrock, Raphael C Pooser, David Jarvis Dean, and Pavel Lougovski, “Cloud quantum computing of an atomic nucleus,” *Phys. Rev. Lett.* **120**, 210501 (2018).
- [11] Matthew Otten and Stephen K Gray, “Recovering noise-free quantum observables,” *Physical Review A* **99**, 012338 (2019).
- [12] Tudor Giurgica-Tiron, Yousef Hindy, Ryan LaRose, Andrea Mari, and William J Zeng, “Digital zero noise extrapolation for quantum error mitigation,” *2020 IEEE International Conference on Quantum Computing and Engineering (QCE)*, 306–316 (2020).
- [13] Andre He, Benjamin Nachman, Wibe A. de Jong, and Christian W. Bauer, “Zero-noise extrapolation for quantum-gate error mitigation with identity insertions,” *Phys. Rev. A* **102**, 012426 (2020).
- [14] Zhenyu Cai, “Multi-exponential error extrapolation and combining error mitigation techniques for nisq applications,” *npj Quantum Information* **7**, 1–12 (2021).
- [15] Youngseok Kim, Christopher J. Wood, Theodore J. Yoder, Seth T. Merkel, Jay M. Gambetta, Kristan Temme, and Abhinav Kandala, “Scalable error mitigation for noisy quantum circuits produces competitive expectation values,” *arXiv preprint arXiv:2108.09197* (2021).
- [16] Suguru Endo, Simon C Benjamin, and Ying Li, “Practical quantum error mitigation for near-future applications,” *Physical Review X* **8**, 031027 (2018).
- [17] Bálint Koczor, “Exponential error suppression for near-term quantum devices,” *Physical Review X* **11**, 031057 (2021).
- [18] William J Huggins, Sam McArdle, Thomas E O’Brien, Joonho Lee, Nicholas C Rubin, Sergio Boixo, K Birgitta Whaley, Ryan Babbush, and Jarrod R McClean, “Virtual distillation for quantum error mitigation,” *Physical Review X* **11**, 041036 (2021).
- [19] Piotr Czarnik, Andrew Arrasmith, Lukasz Cincio, and Patrick J Coles, “Qubit-efficient exponential suppression of errors,” *arXiv preprint arXiv:2102.06056* (2021).
- [20] Bálint Koczor, “The dominant eigenvector of a noisy quantum state,” *New Journal of Physics* **23**, 123047 (2021).
- [21] Mingxia Huo and Ying Li, “Dual-state purification for practical quantum error mitigation,” *Physical Review A* **105**, 022427 (2022).
- [22] Zhenyu Cai, “Resource-efficient purification-based quantum error mitigation,” *arXiv preprint arXiv:2107.07279* (2021).
- [23] Alireza Seif, Ze-Pei Cian, Sisi Zhou, Senrui Chen, and Liang Jiang, “Shadow distillation: Quantum error mitigation with classical shadows for near-term quantum processors,” *arXiv preprint arXiv:2203.07309* (2022).
- [24] Hong-Ye Hu, Ryan LaRose, Yi-Zhuang You, Eleanor Rieffel, and Zihui Wang, “Logical shadow tomography: Efficient estimation of error-mitigated observables,” *arXiv preprint arXiv:2203.07263* (2022).
- [25] Thomas E. O’Brien, Stefano Polla, Nicholas C. Rubin, William J. Huggins, Sam McArdle, Sergio Boixo, Jarrod R. McClean, and Ryan Babbush, “Error mitigation via verified phase estimation,” *PRX Quantum* **2**, 020317 (2021).
- [26] Sam McArdle, Xiao Yuan, and Simon Benjamin, “Error-mitigated digital quantum simulation,” *Phys. Rev. Lett.* **122**, 180501 (2019).
- [27] Xavi Bonet-Monroig, Ramiro Sagastizabal, M Singh, and TE O’Brien, “Low-cost error mitigation by symmetry verification,” *Physical Review A* **98**, 062339 (2018).
- [28] Matthew Otten, Cristian L Cortes, and Stephen K Gray, “Noise-resilient quantum dynamics using symmetry-preserving ansatzes,” *arXiv preprint arXiv:1910.06284* (2019).
- [29] Zhenyu Cai, “Quantum error mitigation using symmetry expansion,” *Quantum* **5**, 548 (2021).
- [30] Yifeng Xiong, Soon Xin Ng, and Lajos Hanzo, “Quantum error mitigation relying on permutation filtering,” *arXiv preprint arXiv:2107.01458* (2021).
- [31] Nobuyuki Yoshioka, Hideaki Hakoshima, Yuichiro Matsuzaki, Yuuki Tokunaga, Yasunari Suzuki, and Suguru Endo, “Generalized quantum subspace expansion,” *arXiv preprint arXiv:2107.02611* (2021).
- [32] Andrea Mari, Nathan Shammah, and William J Zeng, “Extending quantum probabilistic error cancellation by noise scaling,” *Physical Review A* **104**, 052607 (2021).
- [33] Lukasz Cincio, Yiğit Subaşı, Andrew T Sornborger, and Patrick J Coles, “Learning the quantum algorithm for state overlap,” *New Journal of Physics* **20**, 113022 (2018).
- [34] Lukasz Cincio, Kenneth Rudinger, Mohan Sarovar, and Patrick J. Coles, “Machine learning of noise-resilient

- quantum circuits,” *PRX Quantum* **2**, 010324 (2021).
- [35] Prakash Murali, Jonathan M. Baker, Ali Javadi-Abhari, Frederic T. Chong, and Margaret Martonosi, “Noise-adaptive compiler mappings for noisy intermediate-scale quantum computers,” *ASPLOS ’19*, 1015–1029 (2019).
- [36] Sumeet Khatri, Ryan LaRose, Alexander Poremba, Lukasz Cincio, Andrew T Sornborger, and Patrick J Coles, “Quantum-assisted quantum compiling,” *Quantum* **3**, 140 (2019).
- [37] Kunal Sharma, Sumeet Khatri, M. Cerezo, and Patrick J Coles, “Noise resilience of variational quantum compiling,” *New Journal of Physics* **22**, 043006 (2020).
- [38] Piotr Czarnik, Andrew Arrasmith, Patrick J. Coles, and Lukasz Cincio, “Error mitigation with Clifford quantum-circuit data,” *Quantum* **5**, 592 (2021).
- [39] Armands Strikis, Dayue Qin, Yanzhu Chen, Simon C Benjamin, and Ying Li, “Learning-based quantum error mitigation,” *PRX Quantum* **2**, 040330 (2021).
- [40] Ashley Montanaro and Stasja Stanisic, “Error mitigation by training with fermionic linear optics,” *arXiv preprint arXiv:2102.02120* (2021).
- [41] Joseph Vovrosh, Kiran E Khosla, Sean Greenaway, Christopher Self, Myungshik S Kim, and Johannes Knolle, “Simple mitigation of global depolarizing errors in quantum simulations,” *Physical Review E* **104**, 035309 (2021).
- [42] Miroslav Urbanek, Benjamin Nachman, Vincent R Pas-cuzzi, Andre He, Christian W Bauer, and Wibe A de Jong, “Mitigating depolarizing noise on quantum computers with noise-estimation circuits,” *Phys. Rev. Lett.* **127**, 270502 (2021).
- [43] Alejandro Sopena, Max Hunter Gordon, German Sierra, and Esperanza López, “Simulating quench dynamics on a digital quantum computer with data-driven error mitigation,” *Quantum Science and Technology* (2021).
- [44] Daniel Bultrini, Max Hunter Gordon, Piotr Czarnik, Andrew Arrasmith, Patrick J Coles, and Lukasz Cincio, “Unifying and benchmarking state-of-the-art quantum error mitigation techniques,” *arXiv preprint arXiv:2107.13470* (2021).
- [45] Angus Lowe, Max Hunter Gordon, Piotr Czarnik, Andrew Arrasmith, Patrick J. Coles, and Lukasz Cincio, “Unified approach to data-driven quantum error mitigation,” *Phys. Rev. Research* **3**, 033098 (2021).
- [46] M. Cerezo, Andrew Arrasmith, Ryan Babbush, Simon C Benjamin, Suguru Endo, Keisuke Fujii, Jarrod R McClean, Kosuke Mitarai, Xiao Yuan, Lukasz Cincio, and Patrick J. Coles, “Variational quantum algorithms,” *Nature Reviews Physics* **3**, 625–644 (2021).
- [47] Samson Wang, Piotr Czarnik, Andrew Arrasmith, M Cerezo, Lukasz Cincio, and Patrick J Coles, “Can error mitigation improve trainability of noisy variational quantum algorithms?” *arXiv preprint arXiv:2109.01051* (2021).
- [48] Yu Zhang, Lukasz Cincio, Christian F. A. Negre, Piotr Czarnik, Patrick Coles, Petr M. Anisimov, Susan M. Mniszewski, Sergei Tretiak, and Pavel A. Dub, “Variational quantum eigensolver with reduced circuit complexity,” *arXiv preprint arXiv:2106.07619* (2021).
- [49] M. McKerns, L. Strand, T. Sullivan, A. Fang, and M.A.G. Aivazis, “Building a framework for predictive science,” *Proceedings of the 10th Python in Science Conference* (2011).
- [50] Michael McKerns, Patrick Hung, and Michael Aivazis, “mystic: highly-constrained non-convex optimization and uq,” (2009-).
- [51] Alberto Peruzzo, Jarrod McClean, Peter Shadbolt, Man-Hong Yung, Xiao-Qi Zhou, Peter J Love, Alán Aspuru-Guzik, and Jeremy L O’Brien, “A variational eigenvalue solver on a photonic quantum processor,” *Nature communications* **5**, 1–7 (2014).
- [52] W. K. Hastings, “Monte Carlo sampling methods using markov chains and their applications,” *Biometrika* **57**, 97–109 (1970).
- [53] Lukasz Cincio, Kenneth Rudinger, Mohan Sarovar, and Patrick J. Coles, “Machine learning of noise-resilient quantum circuits,” *PRX Quantum* **2**, 010324 (2021).
- [54] Kathleen E Hamilton, Tyler Kharazi, Titus Morris, Alexander J McCaskey, Ryan S Bennink, and Raphael C Pooser, “Scalable quantum processor noise characterization,” in *2020 IEEE International Conference on Quantum Computing and Engineering (QCE)* (IEEE, 2020) pp. 430–440.
- [55] Sergey Bravyi, Sarah Sheldon, Abhinav Kandala, David C McKay, and Jay M Gambetta, “Mitigating measurement errors in multiqubit experiments,” *Physical Review A* **103**, 042605 (2021).
- [56] Filip B Maciejewski, Zoltán Zimborás, and Michał Oszmaniec, “Mitigation of readout noise in near-term quantum devices by classical post-processing based on detector tomography,” *Quantum* **4**, 257 (2020).